THE JOURNAL OF BIOLOGICAL CHEMISTRY
Vol. 257, No. 7, Issue of April 10, pp. 3669-3675, 1982
Printed in U.S.A.

The Horseradish Peroxidase-catalyzed Oxidation of 3,5,3′,5′-Tetramethylbenzidine

FREE RADICAL AND CHARGE-TRANSFER COMPLEX INTERMEDIATES*

(Received for publication, September 21, 1981)

P. David Josephy‡§, Thomas Eling§, and Ronald P. Mason¶

From the §Laboratory of Pulmonary Function and Toxicology and the ¶Laboratory of Environmental Biophysics, National Institute of Environmental Health Sciences, Research Triangle Park, North Carolina 27709

Benzidine and related compounds are well known substrates for horseradish peroxidase/H_2O_2 oxidation. Typically, two different colored products are formed. In this paper, we study the oxidation of 3,5,3′,5′-tetramethylbenzidine. The first colored product is a blue charge-transfer complex of the parent diamine and the diimine oxidation product. This species exists in rapid equilibrium with the radical cation. The radical was observed by ESR spectroscopy, and hyperfine splitting constants were determined. Addition of equimolar hydrogen peroxide yields the yellow diimine, which is stable at acid pH. At less than equimolar peroxide, all four species (diamine, radical cation, charge-transfer complex, and diimine) exist in equilibrium. A theoretical analysis of this redox system is presented, including a determination of the extinction coefficients and equilibrium constant for the nonradical species.

Benzidine is carcinogenic in animals and man (1). It is also mutagenic to bacteria following activation by hepatic microsomes in the Ames test (2).

Peroxidases catalyze the oxidation of a wide variety of substrates, including benzidine and other aromatic amines. Mammalian tissues contain peroxidases; the peroxidatic activity of blood is the basis for the use of benzidine as a reagent for the detection of occult blood. A positive "benzidine test" is indicated by the formation of a blue oxidation product of benzidine (3).

The chemical hazard presented by the use of benzidine as a clinical reagent prompted a search for a less dangerous substitute (4). Holland *et al.* (5) synthesized the compound 3,5,3′,5′-tetramethylbenzidine in which the amino groups are protected by methylation of the adjacent ring positions. This compound proved to be much less hazardous than benzidine itself and even more sensitive as an analytical reagent (5).

The oxidation of aromatic amines by peroxidases has been studied for many years. Saunders (6) has presented a review of this work. Horseradish peroxidase, an enzyme frequently used in these studies, is believed to be capable of both one-electron and two-electron oxidations, depending on the substrate employed. Saunders suggested that the blue oxidation product of benzidine is either its one-electron oxidation product (cation free-radical) or a complex of its two-electron oxidation product (diimine) with the parent diamine. Both of these products are at a net oxidation state halfway between the diamine and diimine, but they are chemically distinct.

The oxidation of *o*-dianisidine (3,3′-dimethoxybenzidine) by horseradish peroxidase/H_2O_2 has been examined (7). Attempts to detect a free radical intermediate using electron spin resonance spectroscopy were unsuccessful. The authors suggested "a direct two-electron oxidation mechanism for horseradish peroxidase acting on *o*-dianisidine ···" and held that "oxidation of dianisidine does not proceed via any detectable semiquinone radical intermediate." This conclusion contrasts with earlier polarographic evidence (8) for the formation of radical intermediates during the electrochemical oxidation of benzidine and dianisidine.

In this paper, we examine the oxidation of the benzidine derivative, 3,5,3′,5′-tetramethylbenzidine, by horseradish peroxidase/H_2O_2. ESR was used to detect and identify the 3,5,3′,5′-tetramethylbenzidine semiquinone-imine cation free radical formed during the oxidation. Optical spectroscopy was used to detect the charge-transfer complex. (See Scheme 1 for structures.)

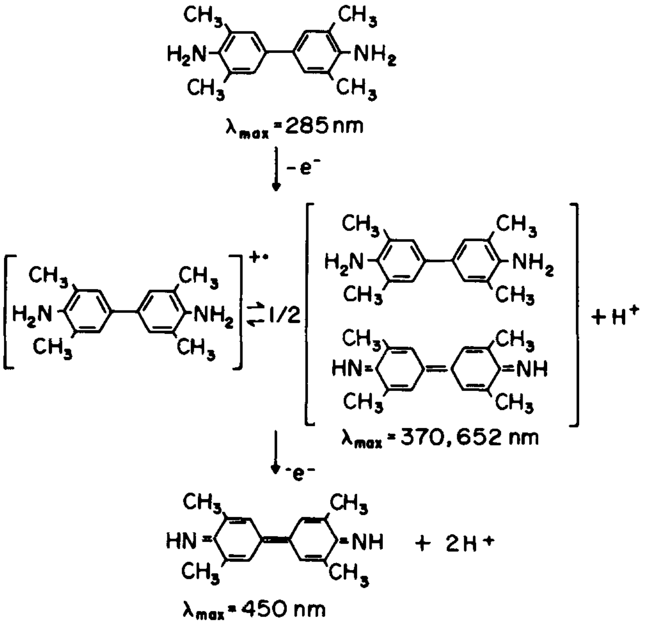

MATERIALS AND METHODS

3,5,3′,5′-Tetramethylbenzidine was obtained from Sigma. (This compound should not be confused with the related benzidine derivative, *N,N,N′,N′*-tetramethylbenzidine.) H_2O_2 (30%) was obtained from Fisher Scientific. Horseradish peroxidase, D_2O, and *o*-dianisidine · 2HCl were obtained from Sigma.

3,5,3′,5′-Tetramethylbenzidine stock solutions were prepared by

---

* The costs of publication of this article were defrayed in part by the payment of page charges. This article must therefore be hereby marked "*advertisement*" in accordance with 18 U.S.C. Section 1734 solely to indicate this fact.

‡ Research Fellow of the National Cancer Institute of Canada.

dissolving the compound in 0.2 N HCl; H_2O_2 and enzyme stock solutions were prepared in H_2O. Incubation mixtures were prepared in 0.2 M acetate buffer, pH 5.0, unless noted otherwise.

Optical spectra were recorded with an Aminco DW-2A spectrophotometer. ESR spectra were recorded with a Varian E-109 or E-104 spectrometer, using an aqueous flat cell and TM_{110} cavity. Further details are given in the figure legends. All experiments were performed at room temperature.

RESULTS

The oxidation of 3,5,3′5′-tetramethylbenzidine by the horseradish peroxidase/H_2O_2 system yields colored products. Incubations turn blue, pass through a green stage, and finally become yellow. The green solution is simply a mixture of the initial blue product and final yellow product. This reaction sequence was studied by optical spectroscopy.

After addition of enzyme to a solution of 3,5,3′,5′-tetramethylbenzidine and H_2O_2, optical spectra were recorded using the auto scan mode of the spectrophotometer (Fig. 1). The UV chromophore of 3,5,3′,5′-tetramethylbenzidine ($\lambda_{max} = 285$ nm) decreases to zero during the reaction, and no new UV peaks appear (data not shown). In the visible region, two new peaks appear initially, at 370 and 652 nm. These peaks grow to a maximum and then decay; they are replaced by a peak at 450 nm. The later stages of the reaction are characterized by a pair of isosbestic points on either side of the 450 nm peak.

In a further experiment, H_2O_2 was titrated into a solution of 3,5,3′,5′-tetramethylbenzidine and enzyme, and the absorbance at 700 nm (blue product) was measured. The resulting titration curve (Fig. 2) shows the formation and subsequent destruction of the blue product. The curve is nearly symmetrical about the midpoint, which corresponds to ½ mol of peroxide/mol of substrate. At the endpoint, reached at approximately equimolar peroxide and substrate, no blue product remains. Beyond this point, the concentration of the yellow product does not increase with additional peroxide. We concluded that the blue product is a one-electron oxidation product of 3,5,3′,5′-tetramethylbenzidine, and that the yellow product is the two-electron oxidation product (diimine).

Two chemically distinct one-electron oxidation products of 3,5,3′,5′-tetramethylbenzidine can be envisaged: the 3,5,3′,5′-tetramethylbenzidine radical cation and the charge-transfer complex of the diamine (electron donor) and the diimine (electron acceptor). The chemical structures of these species are shown in Scheme 1. ESR experiments (reported below) demonstrate the presence of a free radical, but this radical is not necessarily the same as the species responsible for the optical absorption bands since the radical and charge-transfer complex could both exist in equilibrium. Charge-transfer complexes are distinguished by spectral shifts upon dilution caused by the re-equilibration among the electron donor, the electron acceptor, and the charge-transfer complex (9). 3,5,3′,5′-Tetramethylbenzidine was oxidized with enzyme and sufficient peroxide to yield the green stage. Buffer (1 ml) and this mixture (1 ml) were placed in the two chambers of a Yankeelov cuvette. Spectra were recorded before and after mixing (Fig. 3). The distinct change in the spectrum indicates that the equilibrium has shifted from the blue product to the yellow product. This suggests that the blue product is indeed a complex of the parent compound and its imine oxidation product.

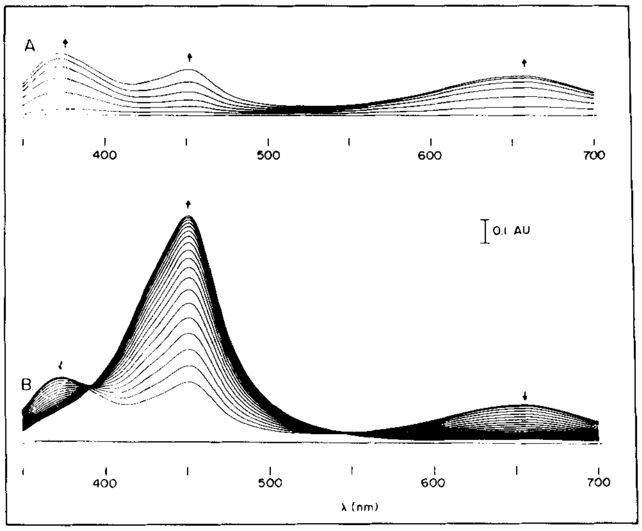

FIG. 1. **Oxidation of tetramethylbenzidine by horseradish peroxidase/H_2O_2:optical spectra.** The incubation mixture contained 10 μM 3,5,3′,5′-tetramethylbenzidine and 15 μM H_2O_2 in acetate buffer, pH 5.0. At zero time, horseradish peroxidase was added (10 ng/ml) and repetitive scanning started (5 nm/s). The first six scans are shown in *A* and the subsequent scans in *B*. *Arrows* indicate the growth and decay of each peak.

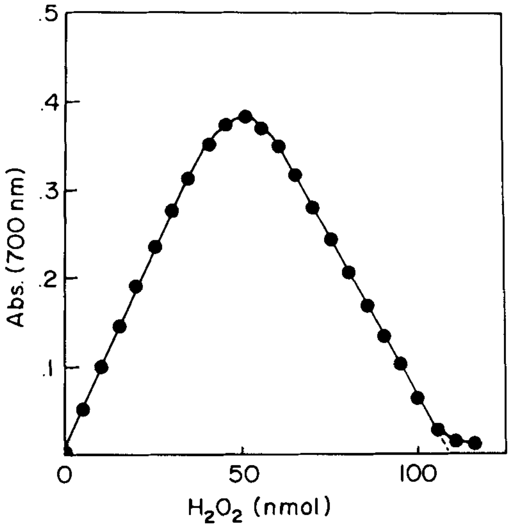

FIG. 2. **Oxidation of tetramethylbenzidine by horseradish peroxidase/H_2O_2:titration curve.** The incubation mixture contained 3,5,3′,5′-tetramethylbenzidine (100 nmol) and horseradish peroxidase (1 mg) in acetate buffer, pH 5.0, 2 ml. H_2O_2 (5 mM) was added in 1-μl aliquots, and absorbance at 700 nm was measured after each addition. The resulting titration curve shows the formation and subsequent destruction of the charge-transfer complex. (See also Fig. A-2.)

ESR experiments were performed, using a ratio of ½ mol of H_2O_2/mol of 3,5,3′,5′-tetramethylbenzidine. The ESR signal developed in a few seconds and was stable for hours. Fig. 4 shows the ESR spectrum observed with the full system. No spectrum was observed in the absence of peroxide, 3,5,3′,5′-tetramethylbenzidine, or enzyme. Horseradish peroxidase, denatured by boiling for 1 h immediately before use, had almost no activity.

To our knowledge, the ESR spectrum of the 3,5,3′,5′-tetramethylbenzidine cation radical has not been reported. The analysis of these spectra was performed with the aid of a computer program for simulation of spectra. The spectra of the cation radicals of benzidine and *N,N,N′,N′*-tetramethylbenzidine (prepared by iodine oxidation in acetonitrile) have been reported (10). These spectra were used as a starting point in our analysis. A summary of these data is given in Table I.

The 3,5,3′,5′-tetramethylbenzidine cation has four distinct types of magnetic nuclei, each characterized by a hyperfine splitting constant. These are: the amine N nuclei (two), the amine protons (four), the protons at the 2 and 4 positions of the rings (four), and the methyl protons (12). Thus, the maximum number of lines possible is $5^3 \times 13 = 1625$. In fact, only about 31 lines can be resolved in Fig. 4. This implies considerable accidental degeneracy.

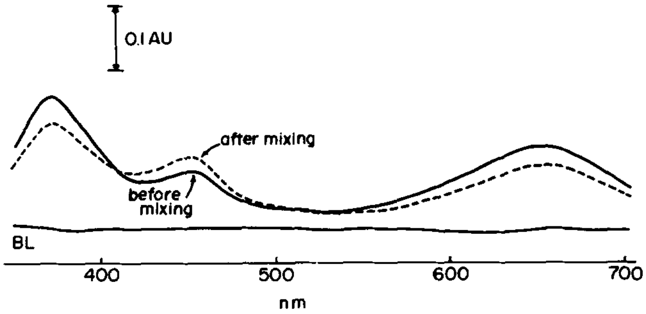

FIG. 3. **Oxidation of tetramethylbenzidine by horseradish peroxidase/H_2O_2:effect of dilution.** A Yankeelov (double-chambered) cuvette was used. One side was filled with 1 ml of acetate buffer, pH 5, containing 3,5,3′,5′-tetramethylbenzidine (25 μM), H_2O_2 (12.5 μM), and horseradish peroxidase (5 μg); the other side contained an equal volume of buffer. Spectra were recorded before and after mixing.

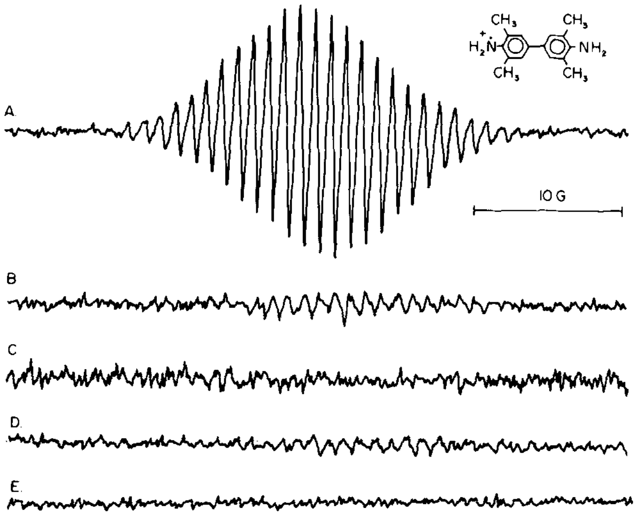

FIG. 4. **ESR spectrum of tetramethylbenzidine cation radical.** The full system (*A*) contained 3,5,3′,5′-tetramethylbenzidine (200 μM), H_2O_2 (100 μM), and horseradish peroxidase (100 ng/ml) in acetate buffer, pH 5. Other spectra are: *B*, heat-denatured enzyme; *C*, no enzyme; *D*, no H_2O_2; *E*, no tetramethylbenzidine. Instrumental conditions were: field, 3366 G; scan range, 50 G; modulation amplitude, 0.13 G; gain, 5×10^4; scan time, 1 h; time constant, 4 s; microwave power, 20 milliwatts.

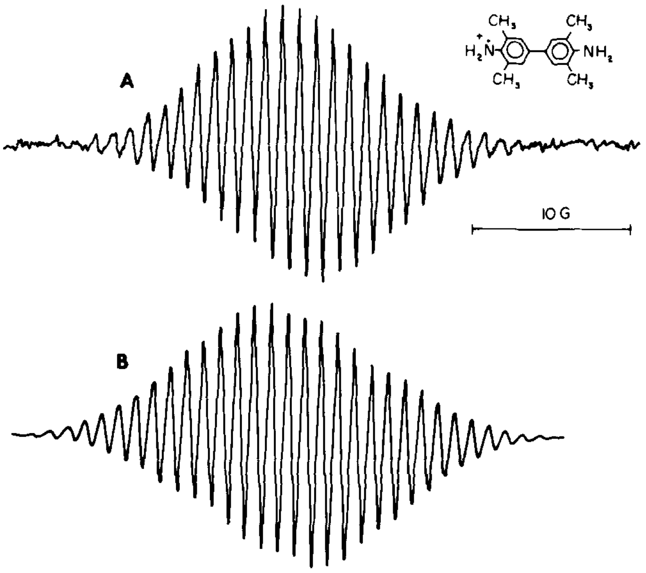

FIG. 5. **Computer simulation of tetramethylbenzidine cation radical ESR spectra.** *A*, experimental spectrum (Fig. 4*A*); *B*, computer simulation. Hyperfine splitting constants were $a^{N}_{NH_2}$ = 3.09 G; $a^{H}_{NH_2}$ = 3.33 G; $a^{H}_{CH_3}$ = 1.08 G; and a^{H}_{ring} = 1.08 G. Line width = 0.45 G.

We considered, first, the amine N and amine H hyperfine splitting constants. If we assume that these are equal, then a 25-line pattern is reduced to a 9-line pattern. Of course, any such assumption can be justified only by a successful analysis of the complete spectrum. The two remaining (proton) hyperfine splitting constants are expected to be much smaller than the amine H and N hyperfine splitting constants. The spacing of the observed lines is remarkably regular. We assumed that this repetitive spacing (about 1.1 gauss) was equal to these two smaller hyperfine splitting constants; the regular spacing can be maintained throughout the spectrum if these hyperfine splitting constants are both close to $1/n$ times the large hyperfine splitting constant, with n an integer. The most promising pattern arises from the assumption that $n = 3$, giving $a^{H}_{NH_2} \simeq a^{N}_{NH_2} \simeq 3 \times a^{H}_{CH_3}$ and $a^{H}_{Ring} \simeq a^{H}_{CH_3}$. This yields a stick spectrum of 41 equally spaced lines. The wing lines of this spectrum are exceedingly weak relative to the central lines and are likely to be missed. Computer simulations of this set of hyperfine splitting constants gave reasonable simulations of the observed spectrum, and slight refinement produced an excellent agreement (Fig. 5). Finally, the deuterium-exchanged spectrum was simulated, using the gyromagnetic

TABLE I

Hyperfine splitting constants of cation radicals of benzidine and derivatives

a, benzidine (Ref. 10); *b*, *N,N,N′,N′*-tetramethylbenzidine (Ref. 10); *c*, 3,5,3′,5′-tetramethylbenzidine (this work).

	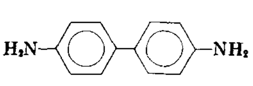 (*a*)	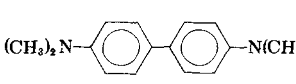 (*b*)	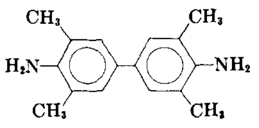 (*c*)
$a^{N}_{NH_2}$	3.39 G	4.81 G	3.09 G
$a^{H}_{NH_2}$	3.52		3.33
$a^{H}_{N(CH_3)_2}$		4.70	
$a^{H}_{Ring\ (3,5,3',5')}$	1.44	1.65	
$a^{H}_{Ring\ CH_3\ (3,5,3',5')}$			1.08
$a^{H}_{Ring\ (2,6,2',6')}$	1.10	0.76	1.08

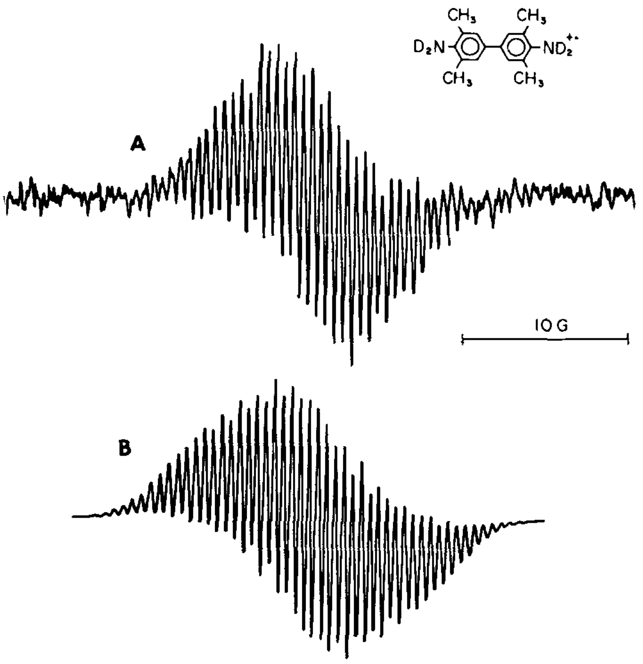

FIG. 6. **ESR spectrum and computer simulation of deuterated tetramethylbenzidine cation radical.** *A*, experimental spectrum. Conditions were as in Fig. 4*A*, except that all solutions were prepared in D_2O. *B*, computer simulation. Hyperfine splitting constants were: $a^{N}_{ND_2}$ = 3.09 G; $a^{D}_{ND_2}$ = 0.52 G; $a^{H}_{CH_3}$ = 1.08 G; and a^{H}_{ring} = 1.08 G. Line width = 0.4 G.

ratios of H and ^2H. This simulation (Fig. 6) is also in close agreement with the observed spectrum and confirms the assignment of the amino N and H hyperfine splitting constants. However, the ring proton (2, 6, 2′, and 6′ positions) hyperfine splitting constants cannot be assigned unambiguously. For example, if these constants are set to zero (leaving 12 rather than 16 protons with a^H = 1.08 G), the resulting simulations are almost identical with those of Figs. 5 and 6. We prefer the assignment of a^H = 1.08 G to ring protons because related benzidines have 2,6,2′6′-ring proton hyperfine couplings on this order (Table I). We concluded that the ESR signal corresponds to the 3,5,3′,5′-tetramethylbenzidine radical cation.

We examined the relationship between the concentrations of the blue product (detected optically) and the free radical (detected by ESR). A series of incubations was prepared, with 3,5,3′,5′-tetramethylbenzidine concentrations ranging from 50 to 500 μM. In each incubation, H_2O_2 was added to give a ratio of ½ mol of peroxide/mol of 3,5,3′,5′-tetramethylbenzidine. The ESR spectrum of each incubation was recorded, using a modified Gilford rapid sampler system so that the flat cell could be filled without removing it from the cavity. Relative ESR signal strength was measured by the peak to peak amplitude of a given line in the spectrum. A second aliquot of each sample was added to an optical cuvette, and the absorbance at 700 nm was measured. Fig. 7 shows the relationship between the two signals; clearly, the radical concentration is proportional to the square root of the concentration of the blue product.

The effect of horseradish peroxidase concentration was also examined. In this experiment (Fig. 8), the concentrations of 3,5,3′,5′-tetramethylbenzidine and H_2O_2 were fixed, and enzyme concentration was varied. The formation of the charge-transfer complex was measured as a function of time following addition of enzyme by recording absorbance at 700 nm. In each case, the final absorbance was the same. Thus, the enzyme affects the rate of the reaction, but not the concentrations of the products formed.

The results shown in Fig. 7 suggest that the blue product (diamine/diimine charge-transfer complex) is in rapid equilibrium with the radical cation. If we represent these species by AA^{2+} and $A^+\cdot$, respectively, then we may write this equilibrium as:

$$2A^+\cdot \rightleftarrows AA^{2+}$$

The two species' concentrations are related by the equilibrium constant:

$$K_{eq} = \frac{(AA^{2+})}{(A^+\cdot)^2}$$

Thus, the radical concentration varies as the square root of the charge-transfer complex concentration, as observed. The equilibrium constant could, in principle, be determined, using quantitative ESR to measure the absolute concentration of the radical. This was not attempted; however, in the following discussion, we will show that the ratio of radical concentration to charge-transfer complex concentration is small (in the concentration regime studied).

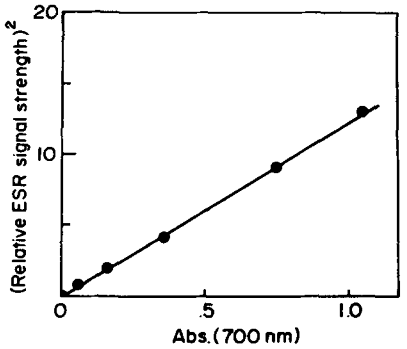

FIG. 7. **Relationship between ESR signal strength and optical absorbance at 700 nm.** A series of incubations was prepared, with 3,5,3′,5′-tetramethylbenzidine concentrations ranging from 50 to 500 μM and horseradish peroxidase 1 ng/ml. In each case, H_2O_2 concentration was one-half of the 3,5,3′,5′-tetramethylbenzidine concentration. From each incubation mixture, an ESR spectrum and an optical spectrum were recorded. ESR signal strength was measured as peak to peak height of a particular line divided by receiver gain. The figure shows a plot of ESR signal strength squared *versus* absorbance at 700 nm.

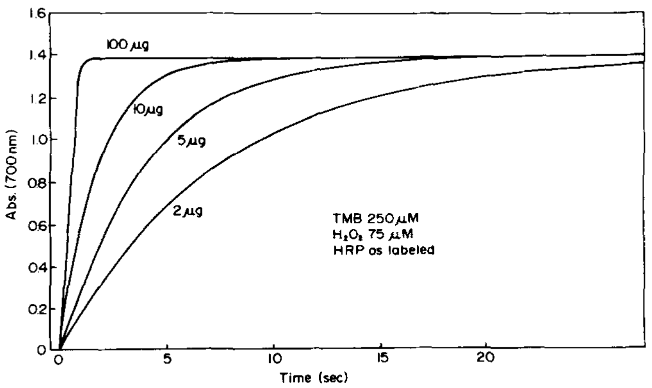

FIG. 8. **Effect of enzyme concentration on 3,5,3′,5′-tetramethylbenzidine oxidation.** 3,5,3′,5′-Tetramethylbenzidine (*TMB*) (250 μM) and H_2O_2 (75 μM) were prepared in acetate buffer, pH 5. This solution (3 ml) was added to a cuvette fitted with a plunger for addition of enzyme. Absorbance at 700 nm was recorded as a function of time; at zero time, the plunger was depressed to start the reaction. The amount of horseradish peroxidase (*HRP*) added (dissolved in 20 μl of buffer) is indicated.

The charge-transfer complex is, itself, in equilibrium with the diamine (A) and diimine (A^{2+}):

$$A + A^{2+} \rightleftarrows AA^{2+}$$

In this case, the equilibrium constant expression is:

$$K'_{eq} = \frac{(AA^{2+})}{(A)(A^{2+})}$$

This equilibrium constant was determined experimentally. The titration experiment of Fig. 2 was repeated, and complete spectra were recorded at each step in the titration. Each of the three absorbing species has an absorption peak substantially free of overlap from the other two species: the diamine parent (λ_{max} = 285 nm), the diimine product (λ_{max} = 450 nm), and the charge-transfer complex (λ_{max} = 652 nm). (The charge-transfer complex absorption peak at 370 nm is less useful due to overlap of the diimine peak.)

The extinction coefficient of each species was determined. The initial concentration of 3,5,3′,5′-tetramethylbenzidine is known, and the absorbance at 285 nm was measured as $\epsilon_{285}^{diamine} = 2.1 \times 10^4$ M^{-1} cm^{-1}. The final concentration of the diimine (following addition of excess peroxide) is equal to the initial concentration of 3,5,3′,5′-tetramethylbenzidine, assuming 100% yield. This allows the determination of the extinction coefficient of the diimine, $\epsilon_{450}^{diimine} = 5.9 \times 10^4$ M^{-1} cm^{-1}.

At each stage of the titration, the concentrations of the diamine and diimine were determined from the absorbances at 285 and 450 nm. If we assume that the radical concentration is negligible, then:

$$(A) + (A^{2+}) + 2(AA^{2+}) = A_0$$

where A_0 is the initial concentration of substrate. The concentration of the charge-transfer complex is given by:

$$(AA^{2+}) = \tfrac{1}{2}\{A_0 - (A) - (A^{2+})\}$$

Thus, from an intermediate stage in the titration, the extinction coefficient of AA^{2+} may be determined: $\epsilon_{652}^{complex} = 3.9 \times 10^4$ M^{-1} cm^{-1}.

Using these values of ϵ, we calculated the sum: $(A) + (A^{2+}) + 2(AA^{2+})$ for each of the first seven steps in the titration, covering a 5-fold range of diamine concentration. Beyond this point, the absorbance due to the diamine became too small for accurate determinations. The sum of the three terms was within 4% of A_0 for each step; this confirms our assumption that the radical concentration may be neglected and gives an estimate of the accuracy of our determination of $\epsilon_{652}^{complex}$.

Finally, the equilibrium constant was determined. In Fig. 9, we plot the concentration of the charge-transfer complex (AA^{2+}) *versus* the product of the concentrations of the diamine and diimine $(A)(A^{2+})$. This plot yields a straight line through the origin, with slope K. Thus, we determined $K'_{eq} = 2.8 \times 10^5$ liters mol^{-1}.

In the Appendix to this paper, we derive an algebraic expression for the concentration of the charge-transfer complex as a function of the number of oxidizing equivalents added per mol of substrate. This expression is based on the law of mass action, and the assumption that the radical concentration is negligible compared to the concentration of the complex. The equilibrium constant K'_{eq} appears as a parameter in this expression, in the form $\hat{K}_c = 1/(A_0 \cdot K'_{eq})$. The parameter $\hat{K}_c$ determines both the shape of the titration curve and the maximum concentration of the charge-transfer complex (at the midpoint of the titration). Using the value of K'_{eq} calculated above and the value of A_0 for the experiment shown in Fig. 2, we obtain $\hat{K}_c = 0.07$; the theoretical expression given in the Appendix yields a predicted maximum concentration of 17 μM for the complex. Experimentally, we measured $A_{700} = 0.38$ at the midpoint of Fig. 2, which gives a concentration of 18 μM, in excellent agreement with the prediction. In Fig. A-2, the data of Fig. 2 are shown superimposed on the theoretical curve for $\hat{K}_c = 0.07$.

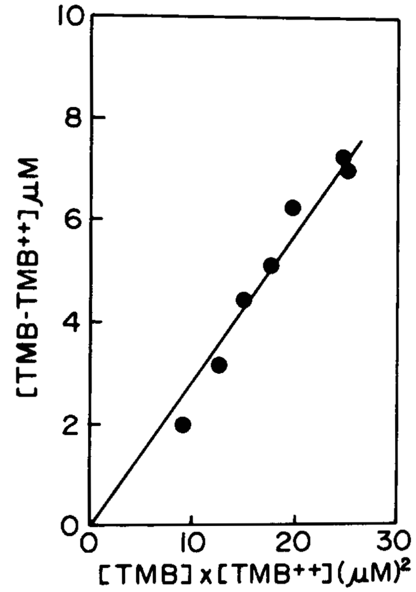

FIG. 9. **Measurement of the equilibrium constant for formation of the charge-transfer complex.** 3,5,3′,5′-Tetramethylbenzidine (*TMB*) (25 μM) and horseradish peroxidase (10 μg) were dissolved in 2 ml of acetate buffer, pH 5. H_2O_2 (5 mM) was added in 1-μl aliquots, and a complete UV-visible spectrum was recorded after each addition. Concentrations of 3,5,3′,5′-tetramethylbenzidine, 3,5,3′,5′-tetramethylbenzidine diimine, and charge-transfer complex were determined from absorbances at 285, 450, and 652 nm, respectively. In the figure, the concentration of the charge-transfer complex is plotted as a function of the product of the concentrations of 3,5,3′5′-tetramethylbenzidine and 3,5,3′,5′-tetramethylbenzidine diimine for the first seven steps in the titration. The equilibrium constant is given by the slope of the straight line through the origin, $K'_{eq} = 2.8 \times 10^5$ liters mol^{-1}.

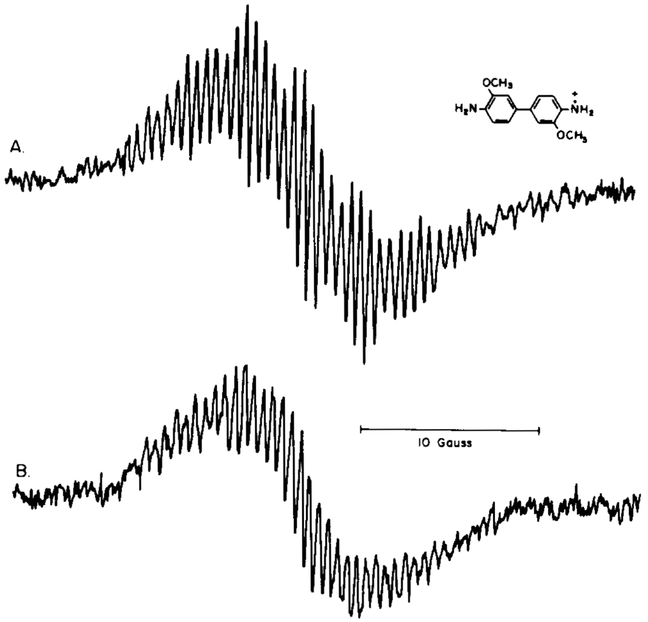

FIG. 10. **Oxidation of *o*-dianisidine by horseradish peroxidase/H_2O_2: ESR spectra.** *A*, the incubation mixture contained *o*-dianisidine (2.1 mM), H_2O_2 (1.0 mM), and horseradish peroxidase (170 ng/ml). Instrumental conditions were: field, 3367 G; scan range, 40 G; modulation amplitude, 0.21 G; gain, 4×10^4; scan time, 8 min; time constant, 0.5 s; and microwave power, 20 milliwatts. *B*, as in *A*, except that all reagents and buffers were prepared in D_2O. Gain, 5×10^4.

We have also studied the oxidation of *o*-dianisidine. In contrast to the earlier report (7), we observed a transient ESR signal during the oxidation of this compound by horseradish peroxidase/H_2O_2 (Fig. 10). The ESR signal was observed in the olive green solution obtained immediately after addition of enzyme. Within a few minutes, the solution turned orange-brown, and the signal disappeared. We believe that the green product is a charge-transfer complex analogous to the blue product of 3,5,3′,5′-tetramethylbenzidine. Again, the charge-transfer complex is in equilibrium with the cation-free radical. However, one or more of the dianisidine oxidation products is unstable. The spectra of the dianisidine radical in H_2O and ^2H_2O (Fig. 10, *A* and *B*) are very similar. Each has a repetitive spacing of about 0.57 gauss. This result can be explained as follows. If $a^{2H}_{NH_2} = 0.57$ gauss, then $a^{H}_{NH_2} = (\gamma_H/\gamma_{^2H}) \times 0.57$ gauss $= 3.7$ gauss. This value is close to that expected for a substituted benzidine cation radical (Table I). Apparently, the accidental equivalence of $a^{2H}_{NH_2}$ and $a^{H}_{\text{ring}\,(2,6,2',6')}$ gives the appearance that the spectrum is essentially unchanged in ^2H_2O buffer. If the wing hyperfine lines could be observed, a decrease in the total width of the spectrum would be apparent in ^2H_2O buffer. Because of the poor signal-to-noise ratio of the experimental spectra and the complexity resulting from the large number of inequivalent nuclei in *o*-dianisidine, a computer simulation of this spectrum was not attempted.

DISCUSSION

A number of investigators (11-13) have suggested the following scheme to describe horseradish peroxidase action:

$$\text{Peroxidase} + H_2O_2 \rightarrow \text{compound I}$$
$$\text{Compound I} + AH_2 \rightarrow \text{compound II} + AH\cdot$$
$$\text{Compound II} + AH_2 \rightarrow \text{peroxidase} + AH\cdot$$

This mechanism implies the formation of substrate-free radicals as intermediates in the oxidation. Indeed, many such radicals have been identified, including those derived from ascorbate, hydroquinone (14), and chlorpromazine (15).

The cation-free radicals of benzidine and several of its derivatives have been observed in chemical systems, such as I_2 oxidation in an organic solvent. Previous investigators failed to detect paramagnetic intermediates during the peroxidase-catalyzed oxidation of dianisidine and suggested that "dianisidine radical is not readily released from the enzyme, but rather serves as electron donor to yield, in a distinct second step, free horseradish peroxidase and dianisidine quinone diimine" (7).

We have shown here that both dianisidine and 3,5,3′,5′-tetramethylbenzidine yield free radicals during peroxidatic oxidation. In the case of dianisidine, the radical is rather short lived. However, the presence of resolved hyperfine structure demonstrates that the radical is free in solution, rather than enzyme bound.

Our analysis of the reaction suggests that the free radical is in rapid equilibrium with both the separated and complexed amine and diimine. Thus, one would expect to detect free radicals whether the initial enzymatic oxidation was one-electron or two-electron in character. Yamazaki (14) has considered this problem explicitly. "If free radicals are formed only (by comproportionation of the oxidized and reduced forms of a bivalent redox molecule), their concentrations cannot exceed the equilibrium value, and the maximum appears at a time when [Ox] = [Red] since the equilibrium is reached in a short time. The free radical remains after the reaction is over, provided that both Ox and Red are present" (14). We believe that this analysis applies to the system described in this paper; thus, it is not possible to decide between a one-electron and a two-electron mechanism for the initial enzymatic step in the reaction without kinetic measurements.

Acknowledgments—We wish to thank Dr. Irwin Fridovich, Biochemistry, Duke University, and Dr. Peter Smith, Chemistry, Duke University, for helpful discussions.

APPENDIX

We consider the oxidation (reduction) of a species, designated A, to its two-electron oxidation (or reduction) product A". We assume that this oxidation proceeds via an intermediate: either a one-electron product (radical) A', or a charge-transfer complex of the parent compound and final product, AA". The two analyses proceed similarly, and will be carried out in parallel.

$$A + A'' \rightleftharpoons 2A' \qquad A + A'' \rightleftharpoons AA'' \qquad (1)$$

If A_0 is the total number of moles of A,

$$[A] + [A'] + [A''] = A_0 \qquad [A] + 2[AA''] + [A''] = A_0 \qquad (2)$$

The equilibrium constants are:

$$K_R = [A']^2/[A][A''] \qquad K_C = [AA'']/[A][A''] \qquad (3)$$

where K_R is dimensionless, and K_C has dimensions: $1 \cdot \text{moles}^{-1}$. Let s be the number of equivalents of oxidation added per mole of A.

Then:

$$[A'] + 2[A''] = sA_0 \qquad 2[AA''] + 2[A''] = sA_0 \qquad (4)$$

Thus:

$$[A''] = \tfrac{1}{2}\{sA_0 - [A']\} \qquad [A''] = \tfrac{1}{2}\{sA_0 - 2[AA'']\} \qquad (5)$$

Substituting (5) into (2) gives;

$$[A] + \tfrac{1}{2}[A'] = A_0\left(1 - \frac{s}{2}\right) \qquad [A] + [AA''] = A_0\left(1 - \frac{s}{2}\right) \qquad (6)$$

and substituting (5) into (3) gives:

$$[A] = [A']^2 \cdot \frac{2}{K_R\,(sA_0 - [A'])} \qquad [A] = [AA''] \cdot \frac{2}{K_C\,(sA_0 - 2[AA''])} \qquad (7)$$

Now, let $[A'] = x_R A_0$

$[AA''] = x_C A_0$

and $\hat{K}_R = 1/K_R$

$\hat{K}_C = 1/(A_0 \cdot K_C)$

Then, substituting the expressions for [A] in (7) into equation (6) yields the quadratic equations:

$$x_R^2\,(4\hat{K}_R - 1) + 2x_R + (s^2 - 2s) = 0 \qquad 4x_C^2 - 4(\hat{K}_C + 1)\,x_C - (s^2 - 2s) = 0 \qquad (8)$$

These expressions may be solved to give the ratio of the intermediate concentration to the total substrate concentration, as a function of s. It is convenient to replace s, which runs from 0 to 2, by t, where t = s-1; thus, t runs from -1 to +1. The solutions are then:

$$x_R = \frac{1 - \sqrt{t^2 + 4\hat{K}_R\,(1 - t^2)}}{1 - 4\hat{K}_R}$$

and

$$x_C = \frac{\hat{K}_C + 1 - \sqrt{\hat{K}_C^2 + 2\hat{K}_C + t^2}}{2}$$

where the signs of the discriminants are fixed by the condition that x = 0 for $t = \pm 1$. Clearly, the solutions are symmetric about the point t = 0.

For any K, the maximum value of x occurs at t = 0, i.e., halfway from A to A". If we denote this value as x max, then:

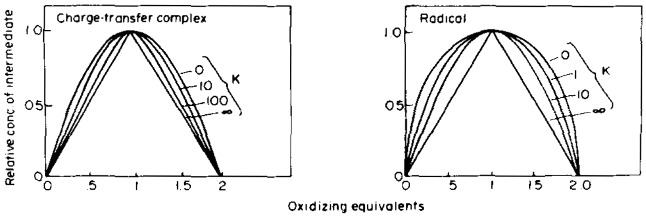

FIG. A-1. **Theoretical titration curves showing formation and destruction of an intermediate in the two-step oxidation (or reduction) of a substrate.** The curves plot relative concentration of the charge-transfer complex (*left*) or free radical (*right*) intermediate, normalized to 1 at the midpoint, as a function of the number of equivalents of oxidation (or reduction) added. The parameter *K* is equal to $A_0 \cdot K_c$ (charge-transfer complex) or K_r (radical), and is the reciprocal of the parameter $\hat{K}$ used in the "Appendix." Derivation of the expressions for these curves is given in the text.

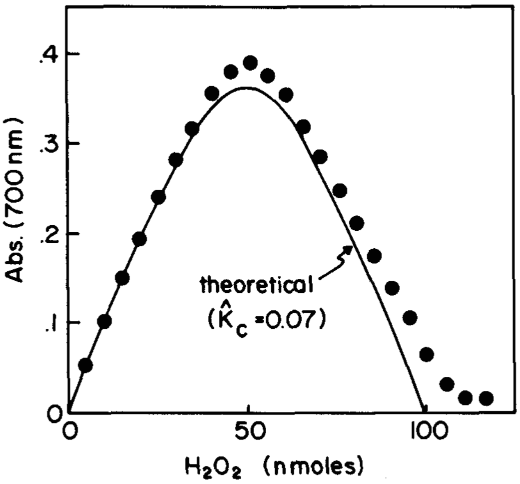

FIG. A-2. **Comparison of theoretical titration curve and experimental results.** The data points are the same as those in Fig. 2. The theoretical curve was calculated as in Fig. A-1 (*left*). The value of $\hat{K}_c$ was determined as explained in the text; this value, and the calculated extinction coefficient of the charge-transfer complex, determine the shape and height of the curve. The width (horizontal scale) was fixed by the assumption of one-to-one stoichiometry (endpoint at 100 nmol of H_2O_2/100 nmol of tetramethylbenzidine). Thus, no correction factors have been applied to the calculated curve.

$$\frac{x_R}{x_{R\,max}} = \frac{1 - \sqrt{t^2 + 4\hat{K}_R (1 - t^2)}}{1 - 2\sqrt{\hat{K}_R}}$$

$$\frac{x_C}{x_{C\,max}} = \frac{\hat{K}_C + 1 - \sqrt{\hat{K}_C^2 + \hat{K}_C + t^2}}{\hat{K}_C + 1 - \sqrt{\hat{K}_C^2 + 2\hat{K}_C}}$$

In Fig. A-1, these functions are plotted against t, for various values of K. These functions provide a quantitative model of the curves obtained by Job's method of continuous variation (16). Such an analysis has been given by Likussar and Boltz (17). A typical application of Job's method involves the complexation of metal ions with organic chelators. The present discussion is distinguished by the fact that the species forming the complex are interconvertible. The case $\hat{K} = 0$ (i.e., equilibrium to the right in equation (1), $K = \infty$) gives

$$x_R = 1 - \|t\|$$

$$x_C = \tfrac{1}{2} (1 - \|t\|)$$

which is a triangular shape. The case $\hat{K} = \infty$ (i.e., equilib. to the left in equation (1), $K = 0$) gives:

$$\frac{x_R}{x_{R\,max}} = \sqrt{1 - t^2}$$

$$\frac{x_C}{x_{C\,max}} = 1 - t^2$$

In principle, then, both the type of intermediate involved in an oxidation, and the value of K, may be determined from a plot of relative concentration of the intermediate (as measured optically or by ESR) as a function of oxidizing equivalents added. The more general case,

$$A + A'' \rightleftarrows 2A' \rightleftarrows AA''$$

involving both a radical and a charge-transfer complex, yields a quartic equation in place of equation (8).

REFERENCES

1. Haley, T. J. (1975) *Clin. Toxicol.* **8,** 13–42
2. Ames, B. N., Sims, P., and Grover, P. L. (1972) *Science* **176,** 47–49
3. Culliford, B. J., and Nickolls, L. C. (1964) *J. Forensic Sci.* **9,** 175–191
4. Garner, R. C., Walpole, A. L., and Rose, F. L. (1975) *Cancer Lett.* **1,** 39–42
5. Holland, V. R., Saunders, B. C., Rose, F. L., and Walpole, A. L. (1974) *Tetrahedron* **30,** 3299–3302
6. Saunders, B. C. (1973) in *Inorganic Biochemistry* Vol. 2, 988–1021 (Eichhorn, G. L., ed) Elsevier, New York
7. Claiborne, A., and Fridovich, I. (1979) *Biochemistry* **18,** 2324–2329
8. Oldfield, L. F., and Bockris, J. O'M. (1951) *J. Phys. Colloid Chem.* **55,** 1255–1274
9. Schlenk, W., and Knorr, A. (1908) *Justus Liebigs Ann. Chem.* **363,** 313–339
10. Horsman, G. (1967) *Colloque Ampère,* Vol. XIV, p. 578, North Holland, Amsterdam
11. George, P. (1952) *Nature* (*Lond.*) **169,** 612–613
12. Chance, B. (1952) *Arch. Biochem. Biophys.* **41,** 416–424
13. Yamazaki, I., Mason, H. S. and Piette, L. H. (1960) *J. Biol. Chem.* **235,** 2444–2449
14. Yamazaki, I. (1977) in *Free Radicals in Biology* (Pryor, W. A., ed) Vol. 3, 183–218 Academic Press, New York
15. Piette, L. H., Bulow, G., and Yamazaki, I. (1964) *Biochim. Biophys. Acta* **88,** 120–129
16. Job, P. (1928) *Ann. Chim. Rome* **9,** 113
17. Likussar, W., and Boltz, D. F. (1971) *Anal. Chem.* **43,** 1265–1272

The horseradish peroxidase-catalyzed oxidation of 3,5,3',5'-tetramethylbenzidine. Free radical and charge-transfer complex intermediates.

P D Josephy, T Eling and R P Mason

J. Biol. Chem. 1982, 257:3669-3675.
